Circular RNAs in the pathogenesis of cancer

Zhao, Xing

DOI:
10.33612/diss.689854111

Chapter 5

Circular ZDHHC11 supports Burkitt lymphoma growth independent of its miR-150 binding capacity

Yichen Liu[1,2], Xing Zhao[1], Annika Seitz[1], Annie A. Hooijsma[1], Reyhaneh Ravanbakhsh[1,3], Sofia Sheveleva[1], Debora de Jong[1], Jasper Koerts[1], Agnieszka Dzikiewicz-Krawczyk[4], Anke van den Berg[1], Lotteke J.Y.M Ziel-Swier[1*], Joost Kluiver[1*]

[1]Department of Pathology and Medical Biology, University of Groningen, University Medical Center Groningen, Groningen, the Netherlands. [2]Cancer Hospital Academy of Medical Sciences and Peking Union Medical College, China. [3]Department of Aquatic Biotechnology, Artemia and Aquaculture Research Institute, Urmia University, Urmia, Iran. [4]Institute of Human Genetics, Polish Academy of Sciences, Poznan, Poland

*Authors share the last authorship

Corresponding authors: Dr. Joost Kluiver, Department of Pathology and Medical Biology, University Medical Center Groningen, Hanzeplein 1, 9700 RB Groningen, The Netherlands. Tel: +31503618075; Fax: +31503619107; Email: j.l.kluiver@umcg.nl

Manuscript submitted

Abstract

We previously showed that MYC promoted Burkitt lymphoma (BL) growth by inhibiting the tumor suppresor miR-150, resulting in release of miR-150 targets MYB and ZDHHC11. The ZDHHC11 gene encodes three different transcripts including a mRNA (pcZDHHC11), a linear long non-coding RNA (lncZDHHC11) and a circular RNA (circZDHHC11). All transcripts contain the same miR-150 binding site region with 18 binding sites. Here we studied the relevance of circZDHHC11 and its miR-150 binding site region for the growth of BL cells. CircZDHHC11 was mainly present in the cytoplasmic fraction in BL cells and its localization was not affected by miR-150 overexpression. Knockdown of circZDHHC11 caused a strong inhibition of BL growth without affecting the expression levels of MYC, MYB, miR-150 and other genes. Overexpression of circZDHHC11 neither affected cell growth, nor rescued the phenotype induced by miR-150 overexpression. Genomic deletion of the miR-150 binding site region did not change the effect of circZDHHC11 knockdown indicating that this region is dispensable for the growth promoting role of circZDHHC11. To conclude, our results show that circZDHHC11 has a strong effect on BL cell growth independent of its ability to sponge miR-150.

Introduction

In our previous work, we have shown expression of a circular RNA (circZDHHC11) derived from the *ZDHHC11* locus in BL[1]. This gene also encodes a protein-coding (pcZDHHC11) and a long non-coding RNA (lncRNA, lncZDHHC11). Knockdown of ZDHHC11 using shRNAs targeting all three transcripts simultaneously resulted in a strong decrease in BL cell growth.

Circular RNAs (circRNAs) are formed through a process called back-splicing of RNA transcripts. The circular shape is generated by a covalent link between the 5' and 3' ends of an RNA molecule. The region where these ends are linked is known as the back-splice junction (BSJ) region[2]. CircRNAs are more stable than linear RNAs because they do not contain free 5' and 3' ends, which makes them resistant to degradation by exonucleases[3]. Thousands of circRNAs have been identified in eukaryotes through RNA sequencing and bioinformatics analyses, which have focused on the identification of reads containing BSJ sequences. About 85% of human circRNAs align to known genes, with the majority being derived from protein-coding exons and a smaller proportion originating from untranslated regions (UTRs) or introns. In addition, circRNAs can be also derived from intergenic regions or from antisense transcripts of known genes[4]. CircRNAs can encompass single or multiple exons, with or without the presence of (part of) introns. The size of circRNAs ranges from 100 nt to more than 4 kb[5].

CircRNA profiling showed cell and tissue type specific expression patterns[6,7], indicating precise regulation and thus supporting functional roles. Most circRNAs are located in the cytoplasm, while a smaller subset of the circRNAs can be found in the nucleus[4]. Characterization of circRNAs has revealed a broad spectrum of different functionalities. One of the best documented functions of circRNAs is to serve as sponges of microRNAs[8]. By competing with other RNA transcripts for binding to microRNAs, circRNAs can indirectly regulate the translation of protein-coding RNA transcripts. The competition between different types of cellular transcripts for binding to miRNAs has been described in a model referred to as the competing endogenous RNA (ceRNA) model[9,10]. Besides binding to microRNAs, circRNAs can also regulate DNA, mRNA and proteins, thereby affecting transcription[11], RNA splicing[12], mRNA stability[13,14] and translation[14-16].

CircRNAs have been implicated in human diseases including different types of cancers[17,18]. Some circRNAs show oncogenic properties[19-21], while others show tumor suppressor activity[22-24]. Relatively little is known about the role of circRNAs in B-cell lymphoma. Initial studies have characterized circRNA expression and/or function in

Burkitt lymphoma (BL), diffuse large B-cell lymphoma (DLBCL), mantle cell lymphoma (MCL) and follicular lymphoma (FL)[1,25,26].

The ZDHHC11 gene contains 18 miR-150 binding sites, which are present in all three transcripts. The postulated functional mechanism of the ZDHHC11 transcripts in regulating growth of BL was to ensure high levels of MYB by binding to miR-150. Enrichment of circZDHHC11 in the AGO2 immunoprecipitated fraction upon miR-150 overexpression was more pronounced than enrichment of pcZDHHC11 or lncZDHHC11. This suggests a strong interaction of circZDHHC11 with miR-150[1]. Based on these findings, we hypothesized that circZDHHC11 might play a dominant role in regulating growth of BL by sponging the available miR-150. In this study, we investigated the relevance of circZDHHC11 and the miR-150 binding site region in regulating growth of BL. We studied the effects of knockdown and overexpression of circZDHHC11 in unmodified BL cells and in miR-150 binding site knockout BL cells.

Materials and Methods

Cell lines and culturing Burkitt lymphoma cell lines ST486 and DG75 and the HEK293T cell line were purchased from ATCC and DSMZ. ST486 was cultured in RPMI 1640 (Lonza BioWhittaker) containing 20% fetal bovine serum (Cambrex Biosciences). DG75 was cultured in RPMI 1640 (Lonza BioWhittaker) containing 10% fetal bovine serum. HEK293T was cultured in DMEM (Lonza BioWhittaker) containing 10% fetal bovine serum. All media were supplemented with 2 mM glutamine, 100 U/mL of penicillin and 100 µg/mL of streptomycin (Cambrex Biosciences). Cells were cultured at 37 °C in a humidified air atmosphere supplemented with 5% CO_2. The origin of the cell lines was confirmed with STR DNA analyses on a regular basis and mycoplasma tests were performed to exclude contamination.

Lentiviral constructs and viral transfections To knockdown expression of circZDHHC11, shRNAs against the BSJ region (Supplemental Fig. 1) were designed and cloned into a miRZip-GFP lentiviral vector. Non-targeting shRNAs were used as controls. To overexpress miR-150, we used a pCDH lentiviral vector containing the miR-150 stem-loop and flanking regions. As a control we included the pCDH vector without an insert (EV). Vectors were all purchased from System Biosciences (Palo Alto). To overexpress circZDHHC11, a PLC5-circ vector based construct was purchased from Geneseed (Guangzhou). Lentiviral particles were generated in HEK293T cells as published previously and were either used directly to infect target cells or stored at -80°C after being harvested[27].

Generation of monoclonal miR-150 binding site depleted ST486 cell line ST486 cells were infected with a lentiviral vector containing two single guide RNAs flanking the miR-150 binding site region and the Cas9 sequence to remove the miR-150 binding site region of the ZDHHC11 locus. This vector was created by inserting a minigene containing both sgRNA sequences as well as the gRNA scaffold for the first sgRNA and the H1 promoter sequence upstream the second sgRNA into the lentiCRISPR-EV-GFP vector (Addgene). As a control, a lentiviral vector with two non-targeting sgRNAs was used. Both vectors contain a GFP reporter, allowing sorting of GFP^+ cells using a MoFlo sorter (BD Biosciences). Cells were plated into 96 wells plates containing 100 µL of 1:8 normal medium:Methocult medium (Stemcell Technologies, Germany), aiming at 1 cell per well. Cultures were subsequently expanded to obtain sufficient cells for isolation of genomic DNA, which was performed with a standard salt-chloroform protocol. To determine deletion of the entire miR-150 binding site region, 100 ng of DNA was used as template in a PCR reaction with 0.033 U/µL of Taq polymerase (Invitrogen) and 0.5 µM of primers in 30 µl reaction volume. After purification of the PCR product using the DNA Clean & Concentrator kit (Zymo Research), it was sequenced by Eurofins Genomics using primers flanking the binding site region. Approximate locations of the primers are indicated in Supplemental Fig. 2, and the sequences are shown in Supplemental Table 1.

Growth competition assays Cells were infected with a lentiviral vector carrying a shRNA against circZDHHC11, the miR-150 or circZDHHC11 sequence and a reporter gene, aiming at an infection percentage of 10-50%. Cells infected with lentiviral vectors containing non-targeting or scrambled sequences were used as controls. Vectors contained GFP, RFP or BFP, and these reporters were used to follow the percentages of infected cells by flow cytometry over time on a BD Accuri C6 Plus Cell Analyzer (BD Biosciences), Calibur flow cytometer (BD Biosciences) or NovoCyte Quanteon flow cytometer (Agilent Technologies). Percentages of infected cells were measured at day 4 post-transfection and monitored tri-weekly for three weeks. Data were analyzed using the FlowJo software (version 10, Treestar). To determine the effect on cell growth, the percentage of GFP/RFP/BFP positive cells at day 4 was set to 100% and the fold difference relative to this starting point was calculated for each time point. The mixed model analysis was performed as previously described to compare the difference of relative GFP/RFP/BFP percentages at day 22 post-transfection[1].

Cell fractionation Cell pellets were washed in 10 mM Tris, pH 8.0, 10 mM NaCl, 2 mM $MgAc_2$, 300 mM sucrose, 0.5 mM DTT, 4 U/mL RNase inhibitor (Ambion/Life Technologies) and EDTA-free protease inhibitor cocktail (Roche). Subsequent cell lysis was performed in the same buffer supplemented with 3 mM CaCl2 and 0.1% NP-40.

After pelleting the nuclear fraction at 1000 x g for 5 min at 4°C, the supernatant was collected as the cytoplasmic fraction. The nuclear fraction was resuspended in 50 mM Tris, pH 8.0, 5 mM $MgAc_2$, 25% glycerol, 0.1 mM EDTA, 5 mM DDT, 20 U/mL RNase inhibitor and EDTA-free protease inhibitor cocktail, and harvested by centrifugation at 1000 x g for 5 min. The fractions were resuspended in Qiazol buffer for analysis by RT-qPCR or in Cell lysis buffer for analysis by Western blot.

RNA isolation, RT-qPCR and PCR Cells or cell fractions were resuspended in 700 µl of Qiazol lysis buffer, and RNA was purified using the miRNeasy micro or mini kit (Qiagen) together with Phase Lock Gel Heavy tubes (5 Prime) according to the manufacturer's protocol. The synthesis and amplification of cDNA were performed as described previously, using 500 ng of RNA[1]. For the subcellular localization experiments, equal volumes of the nuclear fraction and cytoplasm fraction were used for cDNA synthesis. For quantification of the circZDHHC11 levels, 5-10 ng of cDNA was used as input in 10 µL Sybr-Green (Applied Biosystems) qPCR reactions, while 1 ng was used for the other genes. For the quantification of miRNA levels, multiplex miRNA-specific cDNA synthesis and RT-qPCR were performed using the Taqman MicroRNA Reverse Transcription Kit and Taqman MicroRNA Assays (Applied Biosystems) according to the manufacturer's protocol. For validation of the exogenous circZDHHC11 sequence, PCRs were performed with 0.033 U/µL of Taq polymerase (Invitrogen) and an input of 10 ng of cDNA and 0.5 µM of primers in 30 µl reaction volume. After purification of the PCR products using the DNA Clean & Concentrator kit (Zymo Research), they were sequenced by Eurofins Genomics. All primers used are listed in Supplemental Table 1.

Western blot Cells or cell fractions were resuspended in Cell lysis buffer (Cell Signaling) supplemented with 1 mM PMSF. After incubation on ice for 45 minutes and centrifugation for 10 minutes at 14,000 rpm and 4°C, the lysate was collected and the total protein concentration was determined using the Pierce BCA Protein Assay Kit (ThermoFisher Scientific). SDS-PAGE was performed using 10% or 12% polyacrylamide gels and subsequent transfer onto nitrocellulose membranes was done as described previously[27]. Membranes were blocked in 5% ELK in TBST, followed by incubation with antibodies diluted in 5% ELK in TBST. The antibodies used are listed in Supplemental Table 2. Membranes were incubated with SuperSignal West Pico Chemiluminescent Substrate (ThermoFisher Scientific). The proteins of interest were visualized using a ChemiDoc MP scanner and quantified using the Image Lab 6.0 software (BioRad). Protein levels were normalized to GAPDH. For stripping of the membranes, incubation in stripping buffer (25 mM glycine, pH 2.0, 0.001% SDS) for 15 minutes was followed by blocking in 5% ELK in TBST for 15 minutes, after which incubation with antibodies was performed.

Microarray ST486 cells infected with shRNAs against circZDHHC11 or control shRNAs were purified at day 6 post-transfection. RNA was isolated as described above and labeled with Cyanine 3-CTP using the LowInput QuickAmp Labeling kit and Cyanine 3 CTP Dye Pack (both Agilent Technologies) according to the manufacturer's protocol. Cy3-labeled cDNA samples were hybridized on an Agilent SurePrint G3 Human GE 8x60 microarray (Agilent ID 72363) slide overnight. Data were analyzed using GeneSpring GX 12.5 software (Agilent Technologies).

Confirmation of circular RNA structure by RNase R treatment Total RNA (1 µg for each sample) was incubated for 15 minutes at 37 °C with 1 U RNase R (Biosearch Technologies) in a final reaction volume of 15 µL. RNA samples without RNase R were included as controls. After incubation, the RNA was concentrated using a Vivacon® 500 Hydrosart filter (Sartorius, Göttingen, Germany). RNA was replenished to the same volume with H_2O and RT-qPCR was performed to test the abundance of linear and circular RNA using the same volume of RNA as described above.

AGO2 RNA immunoprecipitation Immunoprecipitation of AGO2-containing RISC complexes was performed as described previously with minor modifications[28]. EZview protein G beads (Merck Life Science NV) were pre-blocked using 5% BSA and 2 µg/µL of salmon sperm sonicated ssDNA (Merck Life Science NV), before they were incubated with 10 µg/mL anti-AGO2 antibody (clone 2E12-1C9, Abnova). Mouse anti-IgG antibody was used as negative control. Following the immunoprecipitation procedure, RNA from the total, flow through and immunoprecipitation fractions were isolated and analyzed by qPCR as described above.

Results

Subcellular localization of circZDHHC11

Since the function of circRNAs is related to their subcellular localization, we studied the abundance of circZHHC11 in the nucleus and cytosol (**Fig. 1** and **Supplemental Fig. 3**). We analyzed BL cells with and without miR-150 overexpression to determine whether miR-150 overexpression has an effect on the subcellular localization of the three ZDHHC11 transcripts. Infection of BL cells with lentiviral vectors containing the miR-150 precursor sequence revealed a prominent induction of miR-150 levels in both BL cell lines (**Fig. 1A**). Efficient fractionation was validated by WB and RT-qPCR (**Supplemental Fig. 3**). The pcZDHHC11 and lncZDHHC11 transcripts showed a predominantly nuclear localization with more than 90% of the transcripts residing in the nucleus (**Fig. 1B**). In line with our previous observations that circZDHHC11 and miR-150 strongly interact, both circZDHHC11 and miR-150 are located predominantly in the

cytosol. We did not observe any obvious change in localization of the individual ZDHHC11 transcripts upon miR-150 overexpression.

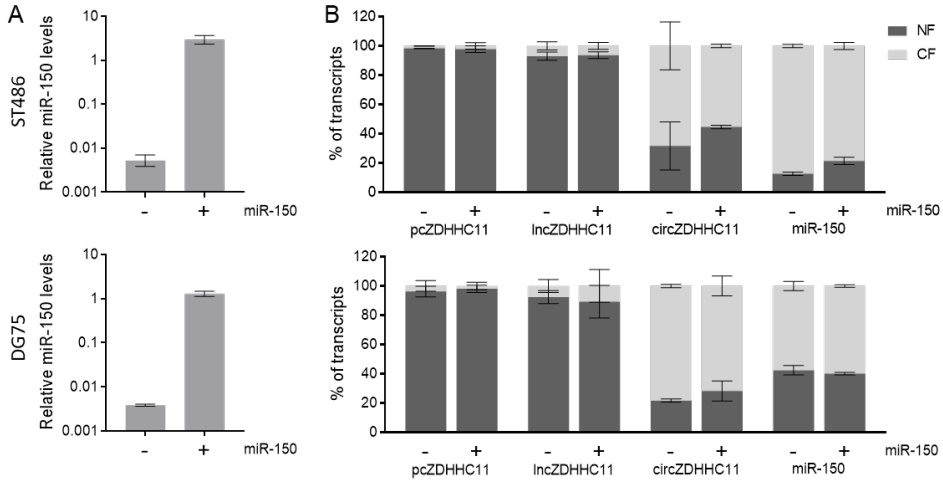

Figure 1. Subcellular localization of the *ZDHHC11* transcripts and miR-150 in BL cells with and without overexpression of miR-150. (A) Exogenous expression levels of miR-150 in ST486 and DG75 upon infection with a lentiviral control vector (-) or miR-150 overexpression vector (+). **(B)** Subcellular localization of the *ZDHHC11* transcripts and miR-150 in the absence (-) or presence (+) of miR-150 overexpression in ST486 and DG75 cells. The fraction of the total RNA present in the cytoplasm (light grey, CF) and nucleus (dark grey, NF) is indicated. Error bars indicate the mean ± SD of two independent experiments.

Knockdown of circZDHHC11 inhibits Burkitt lymphoma cell growth.

To determine the relevance of circZDHHC11 for BL cell growth, we designed shRNAs which specifically knockdown circZDHHC11 without affecting the other ZDHHC11 transcripts. To achieve this, we designed two shRNAs targeting the back-splice junction of the circZDHHC11 transcript (**Supplemental Fig. 1**). Both shRNAs induced a clear knockdown of the circZDHHC11 transcript levels in two BL cell lines without affecting lncZDHHC11 or pcZDHHC11 transcripts (**Fig. 2A**, **Supplemental Fig. 4A**). Knockdown of circZDHHC11 had a strong negative effect on growth in ST486 and a moderate effect in DG75 cells (**Fig. 2B**). In ST486, the decrease in the percentage of GFP^+ cells was 55% for sh1 and 90% for sh2 at day 22. In DG75, both shRNAs result in a decrease of about 40% at day 22. These results showed that circZDHHC11 is important to maintain BL cell growth.

Effect of circZDHHC11 knockdown on gene expression.

To determine whether circZDHHC11 promotes BL growth by regulating the transcript levels of other genes, we performed a genome-wide gene expression analysis upon

circZDHHC11 knockdown in ST486. We observed no significant changes upon knockdown of circZDHHC11 (data not shown). In our previous work, we hypothesized that the ZDHHC11 transcripts ensure high levels of MYB by binding to miR-150, thereby stimulating cell growth[1]. However, MYB protein and transcript levels were not changed upon circZDHHC11 KD, neither did we observe consistent changes for the other network components: MYC and miR-150 (**Supplemental Fig. 4**). Thus, our results suggest that the effect of circZDHHC11 on BL growth does not involve MYB or other components of the network. Together, these data indicate that circZDHHC11 does not affect gene expression levels and more likely acts at the posttranscriptional level.

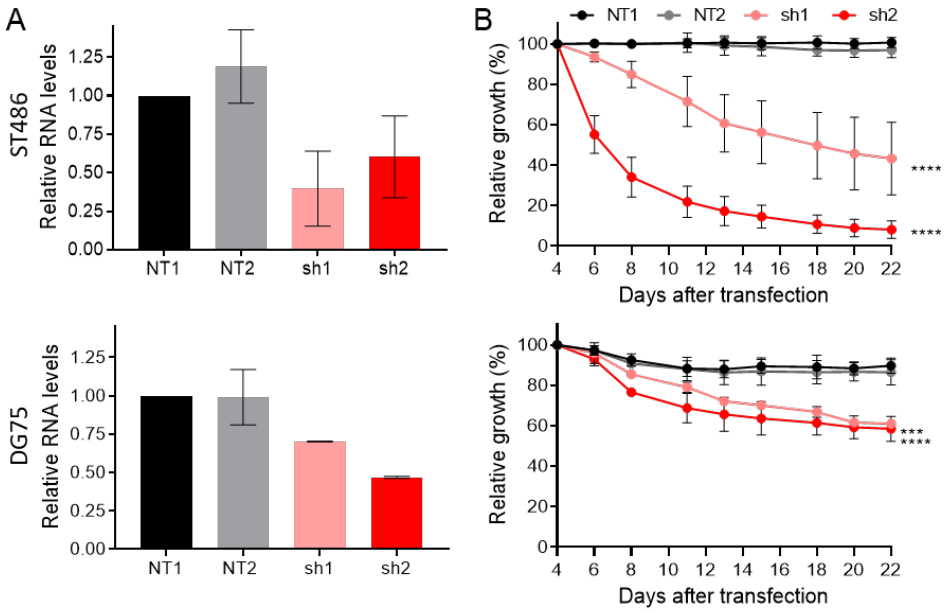

Figure 2. **Knockdown of circZDHHC11 inhibits Burkitt lymphoma cell growth. (A)** The expression of circZDHHC11 was measured by RT-qPCR in ST486 and DG75 cells transfected with lentiviral vectors carrying shRNA (sh1: light red, sh2: dark red) or control (NT1: black, NT2: grey) sequences. Error bars indicate mean ± SD of three (ST486) or two (DG75) independent experiments, and the data were normalized to the NT1 control. **(B)** ST486 and DG75 cells were transfected with lentivirus carrying shRNAs targeting circZDHHC11 or control vectors (colors as in **(A)**). Relative cell growth was assessed by following the percentage of GFP$^+$ cells over three weeks post-transfection (n = 3), with the GFP percentage normalized to day 4 after transfection. Mean ± SD of three independent experiments is shown. Significance was determined by mixed model analysis; *** $p < 0.001$,**** $p < 0.0001$.

circZDHHC11 overexpression does not rescue miR-150 induced inhibition of BL cell growth

We previously showed that miR-150 can strongly interact with the miR-150 BS region in circZDHHC11 and that circZDHHC11 shows a strong increase in AGO2-IP enrichment upon miR-150 overexpression[1]. We therefore wanted to determine whether circZDHHC11 can rescue the miR-150 induced inhibition of BL cell growth. To this end, we generated a lentiviral circZDHHC11 overexpression vector. Effective overexpression of circZDHHC11 was confirmed by RT-qPCR with a fold induction of about 500 in ST486 and 45 in DG75, respectively (**Fig. 3A, D**). Sequence analysis of the exogenous circZDHHC11 including the BSJ region, confirmed proper formation of circZDHHC11 with a correct ligation of the 5' to the 3' ends (**Supplemental Fig. 2A**). The circular nature of the ectopically expressed circZDHHC11 was confirmed upon RNase R treatment (**Supplemental Fig. 2B**). Together, this indicated that the overexpressed circZDHHC11 has the correct sequence and the proper closed-loop structure. The overexpressed circZDHHC11 showed a similar subcellular localization distribution as compared to the endogenous circZDHHC11 and its overexpression did not affect the distribution of the other ZDHHC11 transcripts (**Supplemental Fig. 2C**). GFP competition assays showed no effect on growth of BL cells upon circZDHHC11 overexpression, suggesting that the endogenous circZDHHC11 levels are already sufficiently high to support growth of BL cells (**Fig. 3B, E**).

A double transfection of BL cells with the circZDHHC11 and the miR-150 overexpression vectors revealed that inhibition of cell growth upon miR-150 overexpression was not rescued by overexpression of circZDHHC11 (**Fig. 3C, F**). To confirm that exogenous circZDHHC11 is able to bind miR-150, we performed AGO2 RNA immunoprecipitation upon overexpression of circZDHHC11 in DG75 cells, in the absence or presence of miR-150 overexpression (**Supplemental Fig. 2D**). Overexpression of miR-150 resulted in enrichment of both miR-150 and circZDHHC11 in the AGO2-IP fraction. This indicates that ectopically expressed circZDHHC11 does interact with miR-150. In line with the lack of phenotype rescue upon miR-150 overexpression by circZDHHC11, we also observed that MYB was strongly enriched upon overexpression of miR-150, regardless of circZDHHC11 levels. This indicates that MYB is still targeted by miR-150 despite the circZDHHC11 overexpression. Thus, although circZDHHC11 interacts with miR-150, overexpression of circZDHHC11 does not rescue the growth inhibiting effect of miR-150.

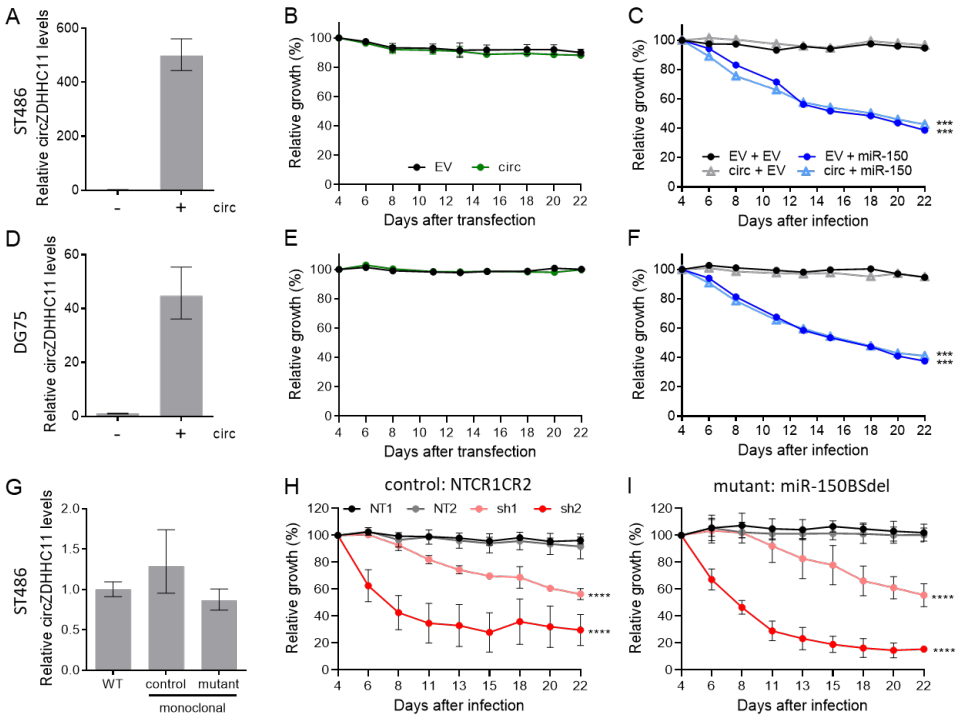

Figure 3. Phenotype of removing the miR-150 binding site region in ZDHHC11 and of circZDHHC11 overexpression. (A) Effective overexpression of circZDHHC11 was obtained in ST486 upon infection with a lentiviral vector containing the circZDHH11 sequence. Data of a representative experiment show mean expression with upper and lower limits, and the levels in absence of circZDHHC11 overexpression are set to 1. **(B)** Relative cell growth of ST486 was assessed upon overexpression of circZDHHC11 (green) or infection with a control vector (black). The percentage of GFP⁺ cells was followed post-transfection for three weeks and the GFP percentage was normalized to day 4 after transfection. Mean ± SD of two independent experiments is shown. **(C)** ST486 cells transfected with the lentiviral vector for circZDHHC11 overexpression (triangles) or control vector (circles) (both with GFP reporter) were transfected with the lentiviral vector for miR-150 overexpression carrying a BFP reporter (dark and light blue) or control (black and grey). Relative cell growth was assessed by following the percentages of BFP⁺ cells in the GFP⁺ fraction over three weeks post-transfection, with the percentages normalized to day 4 after transfection. Significance was determined by mixed model analysis; *** $p < 0.001$. **(D-F)** Same as **(A-C)** in DG75 cells. **(G)** Expression levels of circZDHHC11 in WT ST486 and the monoclonal NTCR1CR2 control and miR-150BSdel mutant cell lines were analyzed by RT-qPCR. **(H-I)** The effect of circZDHHC11 knockdown on growth of the monoclonal NTCR1CR2 and miR-150BSdel cell lines cells (sh1: light red, sh2: dark red, NT1: black, NT2: grey). Relative cell growth was assessed by following the percentage of RFP⁺ cells over three weeks post-transfection from three independent experiments, with the RFP percentage normalized to day 4 after transfection. Significance was determined by mixed model analysis; **** $p < 0.0001$.

The miR-150 binding site region is dispensable for the growth supporting role of circZDHHC11

Since circZDHHC11 overexpression could not rescue the miR-150 induced phenotype, we next studied the importance of the miR-150 BS region for the growth supportive role of circZDHHC11. To this end, we removed the 488 bp miR-150 binding site region from the *ZDHHC11* locus in ST486 cells. A monoclonal cell line (miR-150BSdel) was generated using CRISPR/Cas9 technology with two guide RNAs flanking the miR-150 binding site region in ZDHHC11 (**Supplemental Fig. 5A**). Bi-allelic deletion of the miR-150 binding site region was confirmed by PCR on genomic DNA level and subsequent sequencing of the PCR product (**Supplemental Fig. 5B**). CircZDHHC11 expression levels in the miR-150BSdel monoclonal cell line were similar to the levels observed in unmodified cells and in a monoclonal cell line infected with 2 non-targeting sgRNAs (NTCR1CR2), indicating that circZDHHC11 formation itself was not disturbed by deletion of the miR-150 binding site region (**Fig. 3G**). Knockdown of circZDHHC11 in the miR-150BSdel monoclonal cell line induced a clear negative effect on growth, with a decrease in the percentage of GFP^+ cells that was comparable to the effect observed in the monoclonal control or WT cells (**Fig. 3H-I** and **Fig. 2B**). This indicated that the phenotype induced by knockdown of circZDHHC11 is independent of its ability to interact with miR-150 via the miR-150 binding site region.

Discussion

It has been more than 30 years since the first circular RNAs were described in pathogens[2]. Along with the development of high-throughput sequencing technology and computational pipelines, more and more circRNAs have been identified in different tissues and cell types. Genome-wide expression and functional studies have revealed novel insights and shown a broad spectrum of functionalities. However, the specific role and functional mechanism of the vast majority of circRNAs still needs to be determined. In recent years, more studies have focused on the role of circRNAs in different types of cancer. In this study, we showed that circZDHHC11 supports BL cell growth.

We previously postulated that the role of ZDHHC11 transcripts in the MYC/MYB/miR-150 oncogenic network was through sponging miR-150 and thereby decreasing the miR-150-based regulation of MYB. Based on the more prominent enrichment of circZDHHC11 in the AGO2-IP fraction upon miR-150 overexpression in BL as compared to the linear ZDHHHC11 transcripts, we hypothesized that especially the circZDHHC11 transcript was critical to achieve effective sponging of miR-150[1]. In line with this

hypothesis, we here showed a cytoplasmic localization for both miR-150 and circZDHHC11. The predominant nuclear localization of pcZDHHC11 and lncZDHHC11 argues against a strong interaction of these transcripts with miR-150. Previously we showed that simultaneous knockdown of all ZDHHC11 transcripts reduced growth of BL cells. This was accompanied by a reduction in MYB levels, possibly due to enhanced inhibition of MYB by miR-150[1]. We now specifically knocked down circZDHHC11 and showed that at least the circRNA is one of the ZDHHC11 transcripts that supports BL cell growth. In contrast to the effect of knockdown of all three ZDHHC11 transcripts simultaneously, knockdown of circZDHHC11 did not decrease MYB levels. This might be explained by the much lower endogenous levels of circZDHHC11 as compared to the two linear ZDHHC11 transcripts. Their higher overall levels might still make them efficient miR-150 sponges. It is also possible that the ZDHHC11 protein or the ZDHHC11 lncRNA via direct or other indirect mechanisms can influence MYB levels.

To further understand the growth supporting role of circZDHHC11, we determined whether it could influence gene expression. No effects were observed on genes within the network but also not genome-wide, suggesting that circZDHHC11 exerts its effects at the posttranscriptional level. Ectopic expression of circZDHHC11 did not have an effect on BL cell growth, suggesting that the relatively low endogenous circZDHHC11 levels are sufficient to support growth. It would be interesting to explore a potential growth supporting effect of circZDHHC11 overexpression under suboptimal growth conditions, e.g. low serum, low oxygen or low cell density. Remarkably, overexpression of circZDHHC11 in BL cells overexpressing miR-150 did not result in any rescue of the growth inhibitory phenotype upon miR-150 overexpression. Our results suggest that it is unlikely that this is due to a different subcellular localization or a lack of interaction with miR-150 based on AGO2-IP enrichment of the ectopically expressed circZDHHC11. Altogether these experiments indicate that circZDHHC11 supports growth independent of its interaction with miR-150.

In line with these results, we showed that knockdown of circZDHHC11 in cells lacking the miR-150 binding site region, still inhibited growth of BL cells. Being able to generate monoclonal cell lines with this deletion argues against an important role of the miR-150 binding site region in essential cellular processes. Our results point towards circZDHHC11 functioning independent of sequestering miR-150, potentially by binding to other molecules. This can be driven by the more predominant cytoplasmic or by the less abundant nuclear circZDHHC11 molecules. Since we did not observe any effects at the transcriptional level upon circZDHHC11 KD it seems more likely that circZDHHC11 mainly functions in the cytoplasm.

To further elucidate the role of circZDHHC11, pulldown experiments need to be set up to enable identification of its binding partners. Functions beyond acting as a sponge or as a transcriptional regulator have been described for other circRNAs with a strong miRNA binding domain. For circRNA CDR1as, which is a well-known miR-7 sponge, it was shown that it can stabilize p53 protein independent of its sponge function in glioma[29] and silencing of CDR1as drives IGF2BP3-mediated progression independent of miR-7 in melanoma[30].

Altogether, we showed that the ability of circZDHHC11 to bind miR-150 is not relevant for the growth supportive role of circZDHHC11. This may imply that circZDHHC11 is not part of the MYC-miR-150-MYB-ZDHHC11 network and that the linear ZDHHC11 transcripts are more relevant in this model. The effect of circZDHHC11 on BL cell growth is most likely at the post-transcriptional level, independent of miR-150 binding, potentially via interaction with other cytoplasmic RNA transcripts or proteins. In conclusion, we show that circZDHHC11 is involved in BL cell growth, an effect that is most likely not modulated by binding of miR-150.

Acknowledgements & Funding

This work was funded by grants from Lymph&Co (A.v.d.B and J.K. (Joost Kluiver)), ZeldzameZiekten Fonds (ZZF, J.K. (Joost Kluiver)), the Chinese scholarship council (CSC, Y.L.) and Horizon-Twinning Next-LEVEL funding (A.D.-K. and A.v.d.B).

Author Contributions

Y.L. and L.J.Y.M.Z.-S. conducted experimental work and performed data analysis. Y.L. drafted the manuscript. L.J.Y.M.Z.-S., J.K. (Joost Kluiver), A.D.-K. and A.v.d.B. designed the study and supervised data analysis and writing of the manuscript. X.Z., A.S., A.A.H., R.R., S.S., D.d.J. and J.K. (Jasper Koerts) conducted part of the experimental work. All authors have read and agreed to the published version of the manuscript.

Data Availability Statement

All data generated or analyzed during this study are included in this published article [and its supplementary information files].

References

1 Dzikiewicz-Krawczyk A *et al.* ZDHHC11 and ZDHHC11B are critical novel components of the oncogenic MYC-miR-150-MYB network in Burkitt lymphoma. *Leukemia* 2017; 31:1470-1473.

2 Patop IL, Wust S, Kadener S. Past, present, and future of circRNAs. *Embo J* 2019; 38:e100836.

3 Jeck WR *et al.* Circular RNAs are abundant, conserved, and associated with ALU repeats. *RNA* 2013; 19:141-157.

4 Memczak S *et al.* Circular RNAs are a large class of animal RNAs with regulatory potency. *Nature* 2013; 495:333-338.

5 Szabo L, Salzman J. Detecting circular RNAs: bioinformatic and experimental challenges. *Nat Rev Genet* 2016; 17:679-692.

6 Salzman J, Chen RE, Olsen MN, Wang PL, Brown PO. Cell-type specific features of circular RNA expression. *PLoS Genet* 2013; 9:e1003777.

7 Maass PG *et al.* A map of human circular RNAs in clinically relevant tissues. *J Mol Med (Berl)* 2017; 95:1179-1189.

8 Hansen TB *et al.* Natural RNA circles function as efficient microRNA sponges. *Nature* 2013; 495:384-388.

9 Salmena L, Poliseno L, Tay Y, Kats L, Pandolfi PP. A ceRNA hypothesis: the Rosetta Stone of a hidden RNA language? *Cell* 2011; 146:353-358.

10 Cesana M *et al.* A Long Noncoding RNA Controls Muscle Differentiation by Functioning as a Competing Endogenous RNA. *Cell* 2011; 147:947-947.

11 Li Z *et al.* Exon-intron circular RNAs regulate transcription in the nucleus. *Nat Struct Mol Biol* 2015; 22:256-264.

12 Ashwal-Fluss R *et al.* circRNA biogenesis competes with pre-mRNA splicing. *Mol Cell* 2014; 56:55-66.

13 Xia B, Hong T, He X, Hu XL, Gao YB. A circular RNA derived from MMP9 facilitates oral squamous cell carcinoma metastasis through regulation of MMP9 mRNA stability. *Cell Transplant* 2019; 28:1614-1623.

14 Abdelmohsen K *et al.* Identification of HuR target circular RNAs uncovers suppression of PABPN1 translation by CircPABPN1. *RNA Biol* 2017; 14:361-369.

15 Legnini I *et al.* Circ-ZNF609 Is a Circular RNA that Can Be Translated and Functions in Myogenesis. *Mol Cell* 2017; 66:22-37.

16 Pamudurti NR *et al.* Translation of CircRNAs. *Mol Cell* 2017; 66:9-21.

17 Verduci L, Tarcitano E, Strano S, Yarden Y, Blandino G. CircRNAs: role in human diseases and potential use as biomarkers. *Cell Death Dis* 2021; 12:468.

18 Su M *et al.* Circular RNAs in Cancer: emerging functions in hallmarks, stemness, resistance and roles as potential biomarkers. *Mol Cancer* 2019; 18:90.

19 Verduci L *et al.* The oncogenic role of circPVT1 in head and neck squamous cell carcinoma is mediated through the mutant p53/YAP/TEAD transcription-competent complex. *Genome Biol* 2017; 18:237.

20 Ke Z, Xie F, Zheng C, Chen D. CircHIPK3 promotes proliferation and invasion in nasopharyngeal carcinoma by abrogating miR-4288-induced ELF3 inhibition. *J Cell Physiol* 2019; 234:1699-1706.

21 Okholm TLH *et al.* Circular RNA expression is abundant and correlated to aggressiveness in early-stage bladder cancer. *Cancer Res* 2018; 2:36.

22 Muhammad N, Bhattacharya S, Steele R, Ray RB. Anti-miR-203 suppresses ER-positive breast cancer growth and stemness by targeting SOCS3. *Oncotarget* 2016; 7:58595-58605.

23 Xu JZ *et al.* circTADA2As suppress breast cancer progression and metastasis via targeting miR-203a-3p/SOCS3 axis. *Cell Death Dis* 2019; 10:175.

24 Yang YB *et al.* Novel Role of FBXW7 Circular RNA in Repressing Glioma Tumorigenesis. *Jnci-J Natl Cancer I* 2018; 110:djx166.

25 Dahl M *et al.* Enzyme-free digital counting of endogenous circular RNA molecules in B-cell malignancies. *Lab Invest* 2018; 98:1657-1669.

26 Hu Y *et al.* A circular RNA from APC inhibits the proliferation of diffuse large B-cell lymphoma by inactivating Wnt/beta-catenin signaling via interacting with TET1 and miR-888. *Aging (Albany NY)* 2019; 11:8068-8084.

27 Yuan Y *et al.* miR-24-3p Is Overexpressed in Hodgkin Lymphoma and Protects Hodgkin and Reed-Sternberg Cells from Apoptosis. *Am J Pathol* 2017; 187:1343-1355.

28 Green TM *et al.* High levels of nuclear MYC protein predict the presence of MYC rearrangements in Diffuse Large B-cell lymphoma. *Am. J. Surg. Pathol.* 2012; 36:612-619.

29 Lou J *et al.* Circular RNA CDR1as disrupts the p53/MDM2 complex to inhibit Gliomagenesis. *Mol Cancer* 2020; 19:138.

30 Hanniford D *et al.* Epigenetic Silencing of CDR1as Drives IGF2BP3-Mediated Melanoma Invasion and Metastasis. *Cancer Cell* 2020; 37:55-70.

Supplementary figures and tables

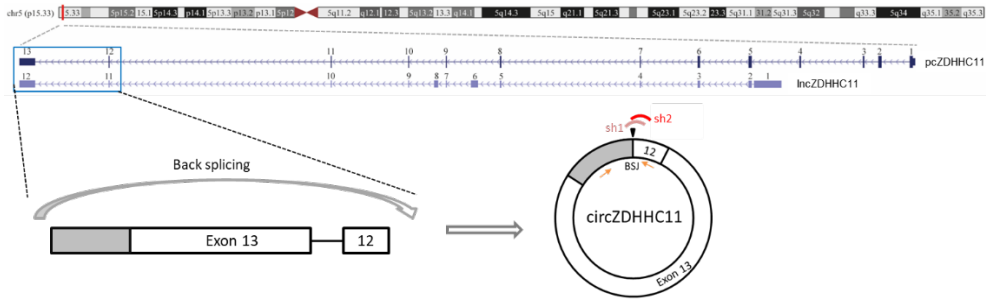

Supplemental Figure 1. ZDHHC11 locus and encoded transcripts. Schematic representation of the *ZDHHC11* locus and the three ZDHHC11 transcripts: protein-coding (pcZDHHC11), lncRNA (lncZDHHC11) and circRNA (circZDHHC11). The circZDHHC11 transcript is formed by back splicing of exon 12, exon 13 and a part of sequence following exon 13. The black triangle indicates the back-splice junction (BSJ) of circZDHHC11. The circZDHHC11 specific shRNAs (sh1 and sh2) targeting the BSJ region are indicated with curved lines, and the RT-qPCR primer set is indicated with the orange arrows.

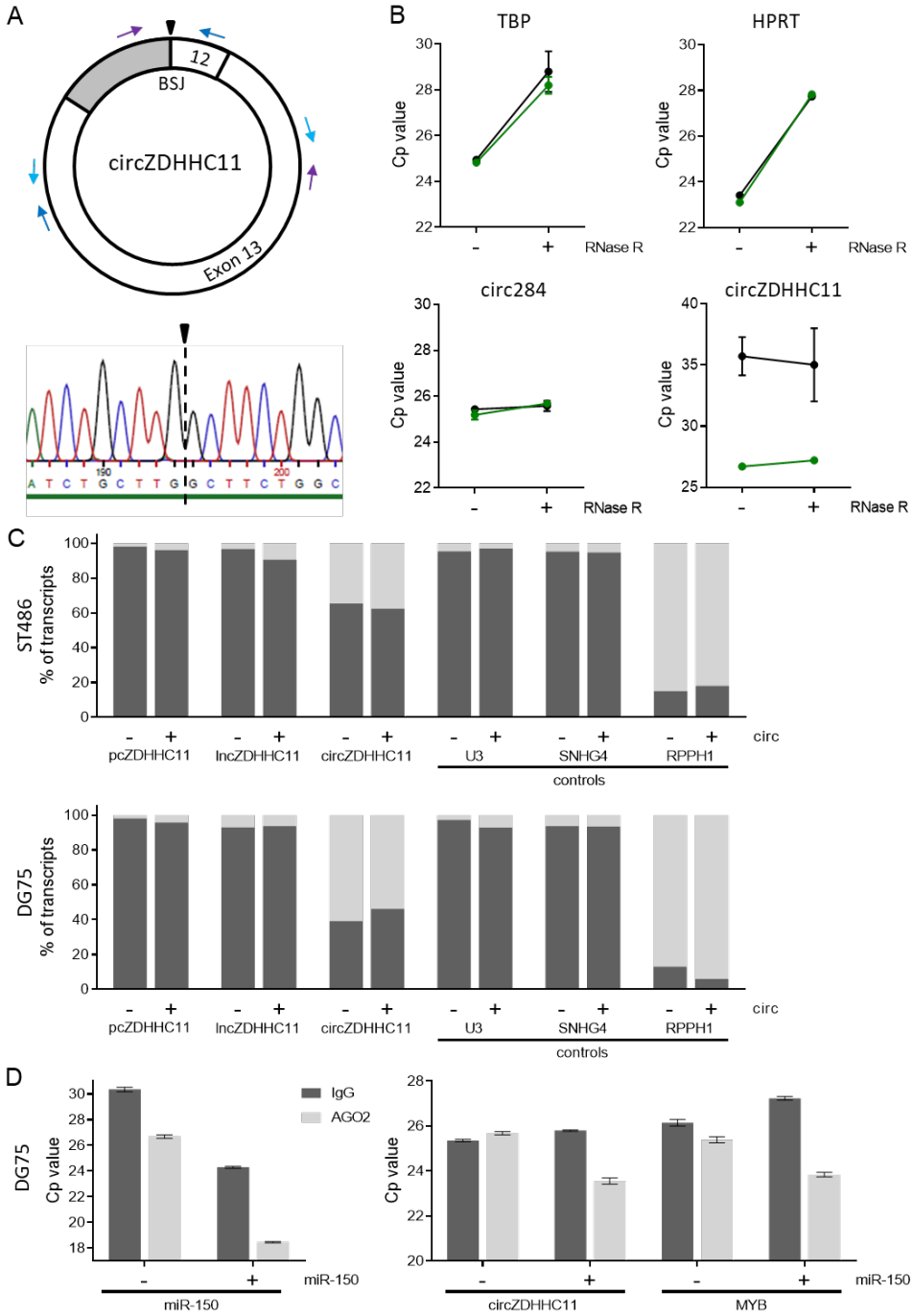

Supplemental Figure 2. Validating overexpression of circZDHHC11. (A) Schematic representation of the circZDHHC11 structure with the arrows indicating the primers used for

sequencing of the circZDHHC11 sequence. Sequence results covering the BSJ showed the expected sequence. The BSJ is indicated by the black triangle. **(B)** Confirmation of the circular nature of the exogenous circZDHHC11 product by RNase R treatment of the RNA samples before RT-qPCR (circZDHHC11 overexpression: green, control: black; - and + indicate the absence or presence of RNase R). Effective RNase R treatment was shown for controls TBP and HPRT. Hsa_circ_0000284 was taken as a positive control for circRNAs being protected from RNase R degradation. Mean ± SD of three experiments are shown. **(C)** Subcellular localization of the *ZDHHC11* transcripts and control RNA transcripts with known subcellular localization in the absence (-) or presence (+) of circZDHHC11 overexpression in ST486 and DG75 cells. The fraction of the total RNA present in the cytoplasm (light grey) and nucleus (dark grey) is indicated. U3 and SNHG4 are located in the nucleus, while RPPH1 is located in the cytoplasm. **(D)** qPCR of the AGO2 (light grey) and IgG (dark grey) immunoprecipitation fractions showing the Cp values for miR-150, circZDHHC11 and MYB upon overexpression of circZDHHC11 and in the absence (-) or presence (+) of miR-150 overexpression.

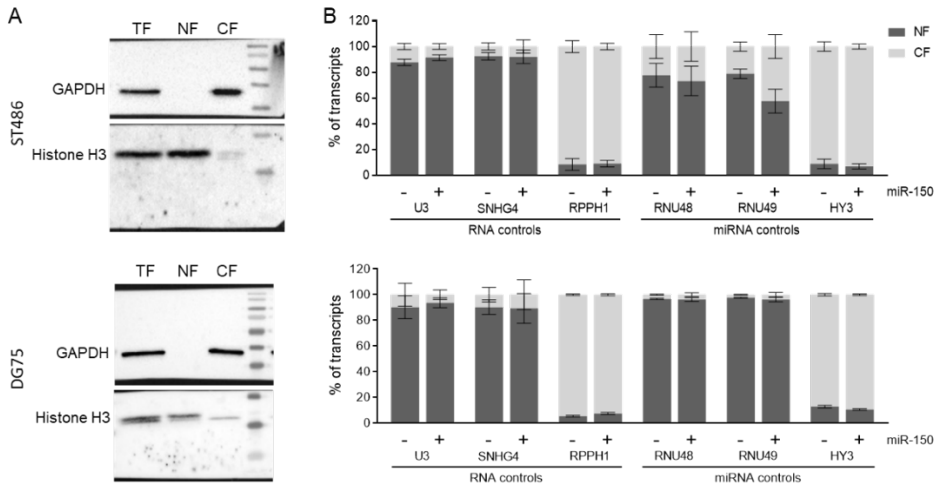

Supplemental Figure 3. Control experiments to determine the efficiency of the cell fractionation for ST486 and DG75 cells. (A) Western blots showing the presence of GAPDH in the cytoplasmic fraction (CF) and histone H3 in the nuclear fraction (NF) of ST486 and DG75 cells. Both proteins are also detected in the total fraction (TF). **(B)** Subcellular localization validation qPCR of control RNA transcripts with known subcellar localization, in ST486 and DG75 cells in the absence (-) or presence (+) of miR-150 overexpression. U3, SNHG4, RNU48 and RNU49 are located in the nucleus, while RPPH1 and HY3 are located in the cytoplasm. The percentage of transcripts located in the cytoplasm (light grey, CF) and nucleus (dark grey, NF) are shown as mean ± SD of two independent experiments.

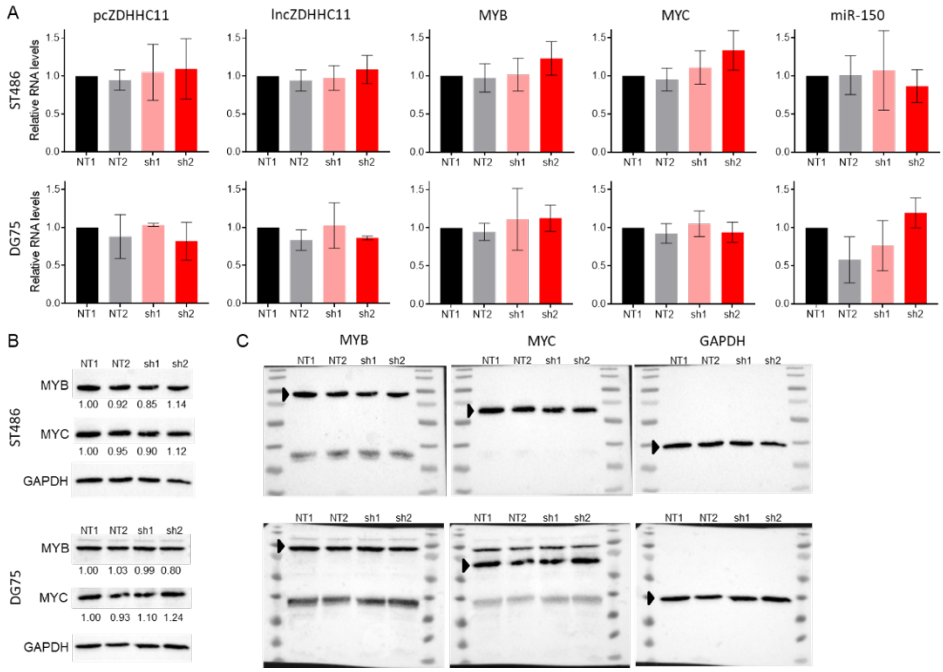

Supplemental Figure 4. Effect of circZDHHC11 knockdown on the expression of other *ZDHHC11* transcripts and network components. (A) Effect of circZDHHC11 knockdown on expression of pcZDHHC11, lncZDHHC11 and other network components in ST486 and DG75. Cells were transfected with lentiviral vectors carrying shRNA (sh1: light red, sh2: dark red) or control (NT1: black, NT2: grey) sequences. Error bars indicated mean ± SD of three (ST486) or two (DG75) independent experiments, and the data were normalized to the NT1 control. **(B)** Western blots showing the effect of circZDHHC11 knockdown on MYB and MYC protein levels. Quantification of MYB and MYC protein levels are normalized to GAPDH. The levels of NT1 were set to 1 for comparison between conditions and cell lines. **(C)** Original pictures of the blots shown in **(B)**. The triangles indicate the position of the specific bands of MYB, MYC and GAPDH. The blots were incubated in the multiple antibody solutions (first with antibody against MYB, secondly with antibody against MYC and finaly with antibody against GAPDH), with stripping of the blots performed in between the incubations.

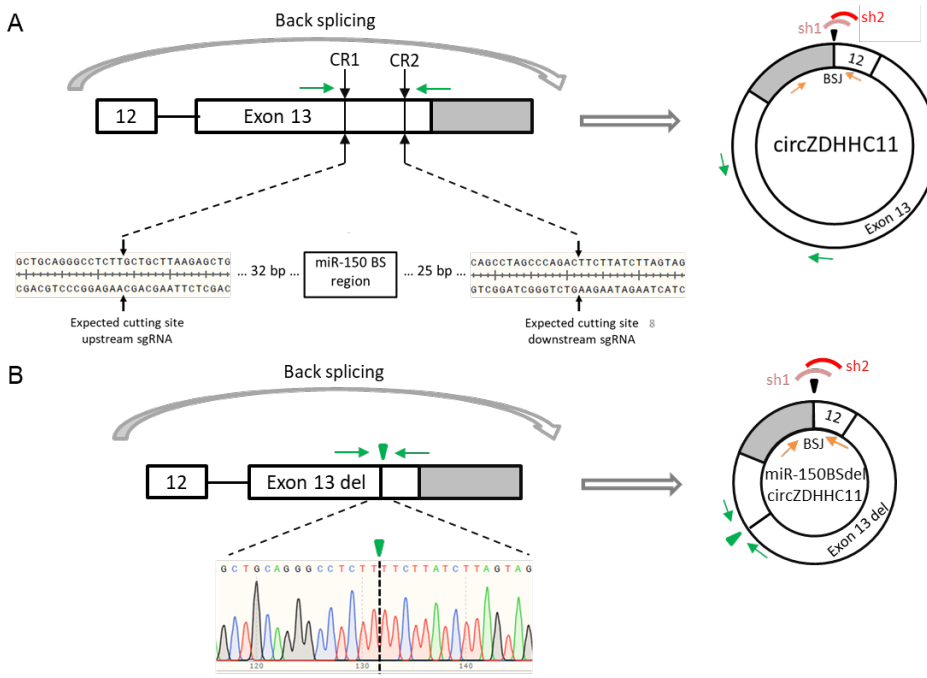

Supplemental Figure 5. Generation of the miR-150BSdel monoclonal cell line. (A) ST486 cells were infected with a lentiviral CRISPR/Cas9 vector containing two single guide RNAs (sgRNA CR1 and CR2, indicated by the two black arrows), which flank the miR-150 binding site (BS) region in ZDHHC11. The expected cutting sites of the sgRNAs in the *ZDHHC11* sequence are indicated with two black arrow sets, with in between the miR-150 BS region. The black triangle indicates the BSJ of circZDHHC11, the red bend lines the circZDHHC11 specific shRNAs and the orange arrow set indicates the positions of the circZDHHC11 specific qPCR primers. **(B)** Sanger sequencing showed the deletion of the miR-150 BS region in the *ZDHHC11* locus of the monoclonal miR-150 BS del cell line. Primers for sequencing are indicated with the green arrow set. The green triangle indicates the junction point after deletion of the miR-150 BS region.

Supplemental Table 1: Oligonucleotide sequences.

Name	Sequence (5'-3')
qPCR primers	
circZDHHC11-F	GGCATCCTCTGTATTTTAATGAACTCT
circZDHHC11-R	GTTGCAGCCAGAAGCCAA
pcZDHHC11-F	TGTCGAGCACTCCCCAGA
pcZDHHC11-R	GCAACGGAAAACGGCTCTC
lncZDHHC11-F	AGCACTTCCTGAAAGCCAGC
lncZDHHC11-R	GAAGAACGCAACAGGCATCG
MYC-F	GCTCATTTCTGAAGAGGACTTGTTG
MYC-R	TTACGCACAAGAGTTCCGTAGCT
MYB-F	CCAACTGTTCACGCAGACCT
MYB-R	CTTCTGATGCTGGTGCCATT
U3-F	AACCCCGAGGAAGAGAGGTA
U3-R	CACTCCCCAATACGGAGAGA
SNHG4-F	AGTAGGGCATCCTTCACCCA
SNHG4-R	CCCTACCCCCATCTGAGCTAT
RPPH1-F	AGCTTGGAACAGACTCACGG
RPPH1-R	AATGGGCGGAGGAGAGTAGT
TBP-F	GCCCGAAACGCCGAATAT
TBP-R	CCGTGGTTCGTGGCTCTCT
HPRT-F	GGCAGTATAATCCAAAGATGGTCAA
HPRT-R	GTCTGGCTTATATCCAACACTTCGT
circ284-F	ATTATGTTGGTGGATCCTGTT
circ284-R	ATATGGTGGGTAGACCAAGA
PCR primers	
circZDHHC11seq-F1	CTTGGCTTCTGGCTGCAAC
circZDHHC11seq-R1	AGCACAGTTAAGCAGGTGGC
circZDHHC11seq-F2	TCTGAGTTTTTCAGCCTAGCCC
circZDHHC11seq-R2	GGGCTCTGTTGTTTCTTGTTGC
circZDHHC11seq-F3	CCAGCATCCATCTCTGTCATCATC
circZDHHC11seq-R3	AATGACTACTAAACAGATGAAAAT
sgCR1CR2-F	CATCCATCTCTGTCATCATC
sgCR1CR2-R	AATGACTACTAAACAGATGAAAAT
sgRNAs	
sgCR1	ATCAGCTCTTAAGCAGCAAG
sgCR2	GTCTACTAAGATAAGAAGTC
sgNTCR1	ACGGAGGCTAAGCGTCGCAA
sgNTCR2	ATCGTTTCCGCTTAACGGCG
shRNAs	
sh1 S	GATCCGCTTGGCTTCTGGCTGCAACTTCAAGAGAGTTGCAGCCAGAAGCCAAGCTTTTTG
sh1 AS	AATTCAAAAAGCTTGGCTTCTGGCTGCAACTCTCTTGAAGTTGCAGCCAGAAGCCAAGCG
sh2 S	GATCCGGCTTCTGGCTGCAACAAGAATTCAAGAGATTCTTGTTGCAGCCAGAAGCCTTTTTG
sh2 AS	AATTCAAAAAGGCTTCTGGCTGCAACAAGAATCTCTTGAATTCTTGTTGCAGCCAGAAGCCG

Supplemental Table 2: Overview of antibodies used for Western blotting.

Name	Dilution	Catalog number, company
rabbit monoclonal anti-c-MYC [Y69]	1:1000	ab32072, Abcam, Cambridge, UK
rat monoclonal anti-c-Myb [ANA236B] (C-terminal)	1:500	ab169111, Abcam, Cambridge, UK
mouse monoclonal anti-GAPDH antibody	1:50000	NB600-502, Novus Biologicals, UK
rabbit polyclonal histone H3 antibody (FL-136)	1:500	sc-10809, Santa Cruz Biotechnology, USA
goat anti-Rabbit immunoglobulins/HRP	1:1000	P0448, Dako, USA
goat anti-mouse immunoglobulins/HRP	1:1000	P0447, Dako, USA
rabbit anti-goat immunoglobulins/HRP	1:1000	P0449, Dako, USA